ELSEVIER

Deep-Sea Research II 52 (2005) 1617–1638

DEEP-SEA RESEARCH
PART II

www.elsevier.com/locate/dsr2

Upper circulation patterns in the Ulleung Basin

D.A. Mitchell[a,*,1], D.R. Watts[a], M. Wimbush[a], W.J. Teague[b], K.L. Tracey[a], J.W. Book[b], K.-I. Chang[c], M.-S. Suk[c], J.-H. Yoon[d]

[a]*GSO, University of Rhode Island, Narragansett, RI 02882–1197, USA*
[b]*Naval Research Laboratory, Stennis Space Center, MS 39529–5004, USA*
[c]*Korea Ocean Research and Development Institute, Seoul, Republic of Korea*
[d]*Research Inst. Applied Mech., Kyushu University, Fukuoka, Japan*

Received 16 July 2002; received in revised form 26 August 2003; accepted 5 September 2003
Available online 27 July 2005

Abstract

Continuous acoustic travel-time measurements from a two-dimensional array of pressure-gauge-equipped inverted echo sounders spanning the entire Ulleung Basin of the southwestern Japan/East Sea between June 1999 and July 2001 are used to examine the upper temperature and current patterns. A new method, referred to as the Residual GEM Technique, interprets the travel-time data into a three-dimensional (x, y, p) time-series of daily, synoptically mapped current and temperature fields. During the two-year measurement period, at least five non-repeating persistent flow patterns are found. The patterns during the first year coincide with changes in the total volume transport through the Korea/Tsushima Strait, while the patterns of the second year do not. The mean temperature of the basin displays strong interannual variability and is correlated with the total Korea/Tsushima Strait transport, with a higher mean temperature in the first year when total volume transport was higher. In addition, a new framework for describing the flow patterns is presented. A newly described cold-core eddy, referred to as the Dok Cold Eddy, is about 60 km in diameter and typically forms southwest of Dok Island when the Subpolar Front loops southward between Ulleung and Dok (Takeshima) Islands and sheds an eddy. The Dok Cold Eddy is highly variable in space and time, and it tends to propagate westward towards the coast of Korea, where it merges with cold waters from the north. Three such propagation events preceed the disappearance of the East Korean Warm Current, which then remains absent between June and November 2000. The Offshore Branch forms by branching in the Korea/Tsushima Strait and is present during much of our two-year observation period.
Published by Elsevier Ltd.

1. Introduction

The Ulleung Basin of the southwestern Japan/East Sea (JES), which is about 2300 m deep, is semi-enclosed by the following shallow topographic

*Corresponding author. Tel.: +1 228 688 4865; fax: +1 228 688 5997.
E-mail address: dmitchel@nrlssc.navy.mil (D.A. Mitchell).
[1]Now at Naval Research Laboratory, Stennis Space Center, MS 39529-5004, USA.

0967-0645/$ - see front matter Published by Elsevier Ltd.
doi:10.1016/j.dsr2.2003.09.005

features: the Korean shelf to the west, the Japanese shelf to the south, the Oki Bank to the east, and the Korea Plateau to the north (Fig. 1). The Ulleung Basin connects to the East China and Yellow Seas along its southern edge through the Korea/Tsushima Strait. The Tsushima Warm Current, the primary inflow to the JES, enters through the strait, which is divided into two channels by Tsushima Island: the western channel with a sill depth of 150 m and a mean depth of 96 m, and the eastern channel with a sill depth of 115 m and a mean depth of 50 m. The combined transport of the Tsushima Warm Current through both channels into the Ulleung Basin averages 2.65 Sverdrups (Teague et al., 2005a; Kim et al., 2004), and contains significant seasonal and interannual variation. As a result of the shallow sill depths, the inflow is confined to the upper few hundred meters and the Ulleung Basin has a distinct two-layer structure (Uda, 1934) and a shallow thermocline.

Historically, the Tsushima Warm Current, which transports warm, salty waters of East China Sea/Kuroshio origin northward, has been thought to split into three distinct branches after passing

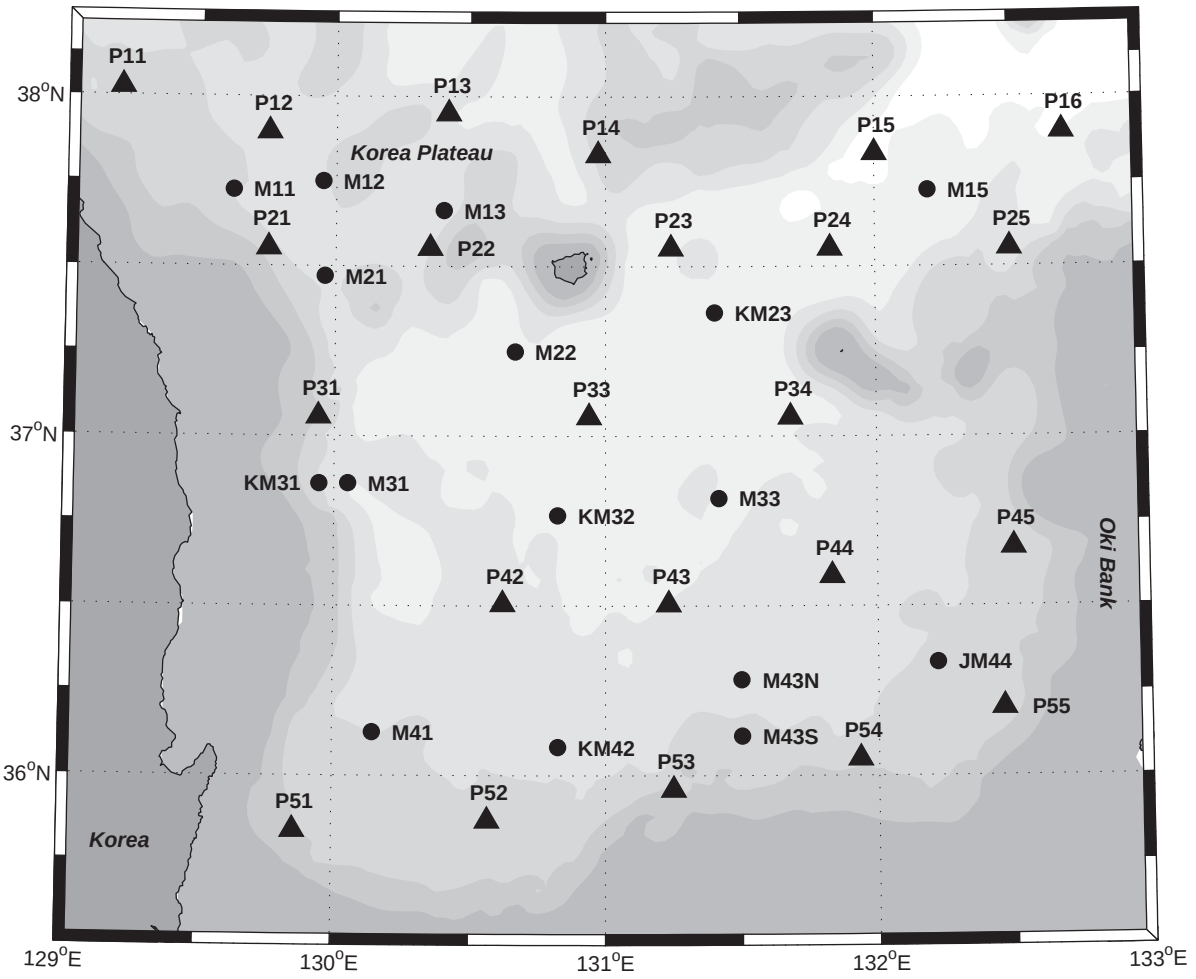

Fig. 1. PIES locations, current meter mooring locations, and bathymetry are shown. The 23 PIES are denoted by solid triangles, with the instrument designation immediately above. The current meter moorings consist of eleven from URI (M moorings), four from KORDI (K moorings), and one from RIAM (J mooring), with mooring designations immediately to the right, except for KM3-1, which is immediately to the left. Depths are in meters, and contour interval is 500 m.

the Korea/Tsushima Straits (Suda and Hidaka, 1932; Uda, 1934). The first branch (''Nearshore branch'' from the Japanese perspective) originates in the eastern channel and flows along the Japanese coast. It is bathymetrically controlled (Yoon, 1982) and is found inshore of the 200-m isobath (Kawabe, 1982a; our observations do not cover this region). The second (Offshore Branch (OB)) and third (East Korean Warm Current, EKWC) branches originate from the western channel, according to Katoh (1994), and were thought to bifurcate from a single branch after entering the Ulleung Basin. (Our observations indicate the bifurcation occurs upstream of the Ulleung Basin.) The second branch, which is highly variable in space and time, is generally thought to flow along the outer edge of Japan's continental shelf slightly seaward of the first branch and exist only from June through August (Suda and Hidaka, 1932; Uda, 1934; Kawabe, 1982a). Senjyu (1999) suggested the OB separated from the EKWC, and Naganuma (1977) found it flowing eastward with an unstable meandering path through the center of the Ulleung Basin. In any case, the OB has large variations (once thought to be seasonal) and its path and variability is not clearly known (Hideaki et al., 1999).

The third branch flows northward along the Korean continental slope until it encounters the southward flowing North Korean Cold Current (NKCC) near 37–38°N, where it separates from the coast and turns eastward forming/joining the Subpolar Front. Numerical models (Kawabe, 1982b; Yoon, 1982) indicate this is a western boundary current controlled by inflow through the western channel of the Korea/Tsushima Strait and the planetary β-effect. When the EKWC separates from the Korean coast it turns anticyclonically and contributes to the Ulleung Warm Eddy (An et al., 1994; Kim et al., 1991), alternately known as the Ulleung Warm Lens (Cho et al., 1990), in the Ulleung Basin. Tanioka (1968) found that 80–90% of the EKWC transport returns southward in the vicinity of Ulleung Island, while other investigators have stated the Ulleung Warm Eddy is the interior of an EKWC meander. The Ulleung Warm Eddy generally occupies an area about 100–150 km in diameter that is marked by high temporal variability (Morimoto et al., 2000). Isoda and Saitoh (1993) observed EKWC intensification when the Ulleung Warm Eddy approached the continental margin, while Lie et al. (1995) showed it to be stationary from December 1992 to September 1993. They also suggested the EKWC may split into a main stream that meanders south around Ulleung Island, and a secondary stream that flows northeast and joins the Subpolar Front.

Alternate views to the branching paradigm also have been introduced. Moriyasu (1972) viewed the Tsushima Warm Current as a single current that meandered and shed eddies. Kawabe (1982a) suggested that branching and the single meander path view could be different stages in one process, the evolution of the Tsushima Warm Current. Naganuma (1985) suggested the two flow patterns may appear alternately.

The Subpolar Front, a thermal boundary between warm southern and cold northern water masses, begins in the northwestern corner of the Ulleung Basin where the EKWC separates from the coast of Korea. The EKWC typically separates from the coast of Korea near 37°N, 129.5°E and turns east near 40°N, 131°E. However, the separation latitude and separation angle of the EKWC relative to the coast of Korea are highly variable, with the separation latitude varying between 36°N and 40°N and the separation angle varying between zero and 90°. Ramp et al. (2005) have suggested that the collision of the northward flowing EKWC and southward flowing NKCC is the dominant process governing the separation of the two currents from the coast. If this is the case, variations in the momentum fluxes of the two currents would account for the alongshore displacement of the separation latitude and the variation in separation angle of the EKWC.

The Subpolar Front meanders energetically (Preller and Hogan, 1998) and sheds many eddies. Generally, there are more eddies south of the front, but many eddies also have been seen north of the front in satellite images (Sugimoto and Tameishi, 1992). Many estimates of the eddy spatial scale have been presented: Baroclinic Rossby Wave theory predicts 100 km (Matsuyama et al., 1990), fractal dimension analysis gives 50–70 km (Miyao, 1994), AVHRR data from 1982 suggest 100 km

(Toba et al., 1982), and analyzed hydrographic data give a range of 30–160 km for eddies and 100–400 km for meanders (Ichiye and Takano, 1988). Stationary warm eddies have been detected in the UB (Lie et al., 1995).

Debate over the current structure in the Ulleung Basin, particularly the "branching" view versus "single meander" view, continues because previous investigations have relied on data sets with limited spatial coverage and poor temporal resolution. The data sets analyzed have typically been single hydrographic surveys of limited spatial extent or regional hydrographic surveys (covering less than half of the basin) repeated every 2–3 months. The debate over which view of the circulation is appropriate stems from multiple interpretations of these data sets, because a branching structure and a meandering structure are generally indistinguishable in these limited data sets. Thus, interpretations of these earlier data sets have been inconclusive. Furthermore, due to the non-synoptic nature and limited spatial coverage of these data sets, the Dok Cold Eddy (an important circulation feature of the Ulleung Basin newly described in this paper) was overlooked. One thing all investigators have agreed upon is the highly variable nature of the upper circulation in the Ulleung Basin. In this paper, we will present a new perspective on the circulation structure, on the path of the Subpolar Front in the Ulleung Basin, on the shape and variability of the Ulleung Warm Eddy, on the path and variability of the OB, and on the formation and behavior of the Dok Cold Eddy, based on a mapping of the observed upper current field derived from a basin-wide, two-year time-series of data collected in the Ulleung Basin.

2. Instrumentation

Twenty-five pressure-gauge equipped inverted echo sounders (PIES) were deployed during June 1999 as an approximate 5×5 array with 50–60 km spacing covering a 220×240 km region in the Ulleung Basin (Fig. 1). Twenty-three were recovered in June–July 2001, with crab fishing probably responsible for the two losses. Instrument spacing was selected to allow coherent mapping of mesoscale features, based on a correlation length scale of 100 km estimated for upper layer features using Rossby wave theory (Matsuyama et al., 1990).

A PIES measures vertical acoustic travel time (τ) with an accuracy of 1.6 ms and a resolution of 0.05 ms, abyssal pressure (P) with a resolution of 0.001 dbar, and an accuracy of 0.1–0.3 dbar, and temperature (used to correct the Digiquartz pressure transducer's temperature sensitivity) with an accuracy of 0.15 °C and a resolution of 0.0007 °C. All measurements were recorded hourly.

Seventeen Aanderaa Recording Current Meter 8 (RCM8) moorings were concurrently deployed at approximately the midpoints between the PIES (Fig. 1). Eleven were maintained by the University of Rhode Island (URI), four by the Korean Ocean Research and Development Institute (KORDI), and one by the Research Institute of Applied Mechanics (RIAM) of Kyushu University. On each mooring there was an RCM8 positioned about 25 m above the bottom, high enough that it should be above the benthic boundary layer. The RCM8 records current speed and direction, and temperature. For the JES array, magnetic variation, used to correct from magnetic to true direction, ranged from 7.5° to 8.1°. The URI and RIAM data were recorded at one-hour intervals while the KORDI data were recorded at one-half-hour intervals. Additional current meters were installed at shallower depths on the KORDI mooring EC1 (KM2-3) (Chang et al., 2002). The RCM8 and bottom pressure data are discussed in Teague et al. (2005b).

During the deployment cruise, 25 XBT casts were taken, one at each PIES site immediately following the PIES launch. On the recovery cruise 25 CTD casts were taken, one at each PIES site approximately 24 h prior to the PIES recovery.

3. Data processing

Novel difficulties were encountered during the processing of the PIES data, specifically, P and τ jumps (offsets) on 11 sites, and complicated sensor drifts on six sites. The jumps presumably resulted from the instruments being displaced to different

depths by the deep crab fishing activity in the region. The P and τ jumps always occurred simultaneously at an individual site and had relative displacements consistent with vertical movement of the instrument ranging from centimeters to tens of meters, either upward or downward. The complicated drifts all occurred on five pressure sensors with similar serial numbers, suggesting the possibility of a bad batch. These sensors have since been retired. Three of the records had the added complication of a very strong drift at the beginning of the record that trended in opposition to the remainder of the record. In order to produce coherent maps of P and τ, these jumps and drifts were estimated and subtracted from the records. This section provides a brief description of the processing scheme applied to the PIES data.

The 23 P records all bore a striking resemblance to one another due to the dominance of a basin wide response to atmospheric forcing (see Park and Watts, 2005). The first processing step was the selection of "clean" records without jumps and with sensor drifts less than 0.1 dbar/yr. The three selected records were then dedrifted with the exponential/linear method of Watts and Kontoyiannis (1990), then detided using tidal response analysis (Munk and Cartwright, 1966). The basin average $\bar{P}_b(t)$ was simply the average of these three dedrifted/detided P records.

The next step removed jumps (ΔP) from 11 P records through the following iterative process designed to increase the signal-to-noise ratio. There were a total of 33 jumps among the 11 affected PIES instruments, with each jump occurring within a 1–3 h window (1–3 measurements). The tidal signal was dominant over this short timescale, and it was used as an initial prediction of what the pressure would be if the jumps did not occur. Jumps were treated one at a time, with ΔP calculated as the pressure of the final jump measurement minus the pressure predicted by the tide at the same point, with all subsequent measurements adjusted accordingly. The tide was then calculated from this preliminary "dejumped" record using tidal response analysis, and then a residual record was created by removing the tidal signal and $\bar{P}_b(t)$ from the original P record. An improved estimate of the jump was then removed from this weakly varying residual record by setting the measurements affected by the jump equal to the measurement prior to the jump and adjusting the remainder of the record accordingly.

Fourteen of the 20 "unclean" records had simple drifts and were dedrifted with the Watts and Kontoyiannis method. The other six had complicated drifts and were dedrifted by fitting, in the least-squares sense, double-exponential/linear curves to the records. Four of these records required fitting separate curves to different portions of the record due to strongly opposing trends, with the constraint they be equal at the break points. The calculated drift curves were then removed and the records detided using tidal response analysis.

The τ processing was simpler, because there was no sensor drift, and only required the removal of τ jumps, all of which coincided with pressure jumps. Because the pressure jumps could be estimated with greater accuracy, the τ jumps were calculated as: $\Delta\tau = 2\Delta Z/c$, where c is the speed of sound at the instrument depth, and $\Delta Z(\mathrm{m}) = \Delta P(\mathrm{dbar})/1.01$ is the change in instrument depth. The jumps were removed by subtracting $\Delta\tau$ from all measurements after the jump.

The final steps in the P and τ processing were spike removal and low-pass filtering. The P records exhibited sporadic spikes which were removed. Spike removal was especially important in the τ records, because many of the PIES sites recorded echo returns that arrived earlier than expected for sea-surface echoes. These early echoes exhibited a diurnal pattern consistent with vertical migration of zooplankton, fish, or squid, rising from 225 m at night to the surface during the day. Both P and τ records were low-pass filtered with a fourth-order Butterworth filter run forward and backwards to avoid introducing phase shifts. A 120-h cutoff frequency was used, and all low-pass records were output once per day at 1200 UT.

4. Analysis methods

The JES is characterized by a spatially varying seasonal signal that extends through the depth of

its shallow thermocline. In order to interpret the PIES τ data and to separate eddy variability and interannual variability from seasonal climatology, it was necessary to extend the GEM technique originally developed by Meinen and Watts (2000) for the Newfoundland Basin and Watts et al. (2001) for the Subantarctic Front. The GEM technique is a method for determining oceanic vertical profiles from vertically integrated quantities, based on available hydrographic data. The extension was accomplished by combining the Navy's MODAS (Fox et al., 2002) static climatology, which implicitly contains the seasonal signal, with the standard GEM technique. We refer to this new method as the Residual GEM Technique (Mitchell et al., 2004). The Residual GEM Technique estimates the temperature at 100 dbar with an accuracy of 1.5 °C, and geopotential height at the surface relative to 500 dbar with an accuracy of 2.44 cm (Mitchell et al., 2004).

This study, as in many previous studies (Katoh, 1994; Kawabe, 1982a; Moriyasu, 1972; Tanioka, 1968), examines the evolution of the temperature structure at 100 dbar. The 100-dbar pressure level was selected for two reasons: (1) it is below the seasonally dominated surface layer, and (2) it is within the main thermocline. We use the temperature contours at 100-dbar as a proxy for the geostrophic streamfunction, and thus the current structure, at 100 dbar. Tanioka (1968) and Moriyasu (1972) have shown that the horizontal temperature distribution at 100 dbar is well correlated with the dynamic topography at the surface relative to 500 dbar, and thus the geostrophic streamfunction.

5. Results

During June 1999 to July 2001 the upper circulation pattern in the Ulleung Basin is dominated by a sequence of quasi-stable patterns. The five dominant patterns are portrayed in Fig. 2 by maps of the mean temperature at 100 dbar averaged over the duration of each pattern. Patterns 1 and 2 occurred during the first year of the deployment when the basin was predominantly warm, and the EKWC passed out of the Ulleung Basin on northerly and northeasterly routes, respectively. Patterns 3, 4, and 5 occurred in the second year when the basin became cooler and the Subpolar Front was found within the Ulleung Basin. The EKWC was absent in pattern 3, it returned along the coast to about 37°30′N and then flowed eastward. In patterns 4 and 5, the Subpolar Front developed a large meander trough. The Ulleung Warm Eddy displayed a rich variety of behaviors throughout the two-year period, including fluctuations in size, shape, and position. The OB, though highly variable in space and time, was present almost continuously. Also notable was the existence of a cold-core eddy south of Dok Island that displayed high spatial and temporal variability. Because the Nearshore Branch is found inshore of the 100 m isobath (Kawabe, 1982a), and our shallowest PIES are located at about 1000 m, the Nearshore Branch and its fraction of the Korea/Tsushima Strait transport is not considered here.

5.1. Pattern 1: Ulleung (Warm) Eddy/Dok (Cold) Eddy

Pattern 1 had four major features and was observed from June 15, 1999 (when the array was deployed) until September 30, 1999 (Figs. 2 and 3). The first feature was a strong temperature gradient perpendicular to the Korean coast associated with the EKWC. The EKWC flowed northward adjacent to the coast of Korea until it converged with the NKCC at 37°N and separated from the coast. The second feature was a bifurcation of the EKWC near Ulleung Island at 37°30′N, with the majority of the flow exiting the Ulleung Basin to the north. The remainder turned south along 131°E, forming an elliptical loop of current with a 250-km north/south major axis and a 90-km minor axis. The loop warmed throughout the pattern, reaching a maximum of 15.12 °C on October 22, 1999. By August 26, the neck pinched closed forming the Ulleung Warm Eddy eddy centered near 36°30′N, 130°40′E. The third feature was a temperature gradient in the southeast corner associated with the OB. Finally, there was a persistent cold-core eddy, henceforth called the Dok Cold Eddy, adjacent to the OB centered

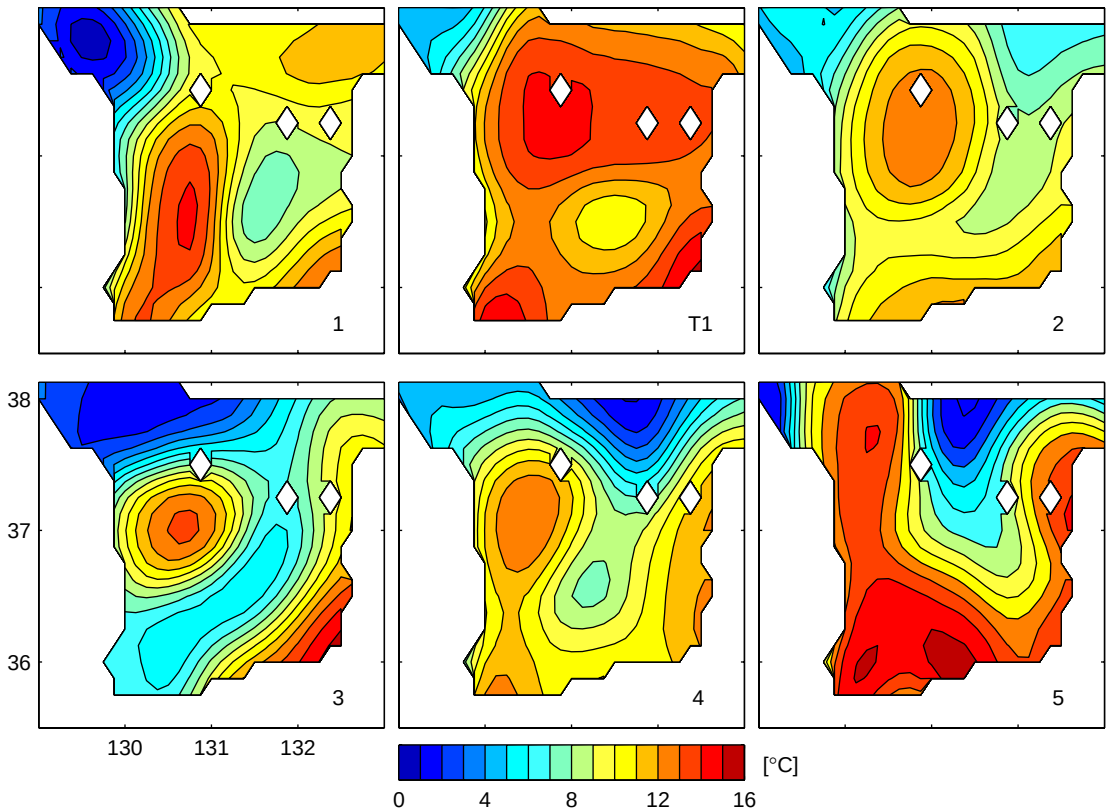

Fig. 2. Mean temperature at 100 dbar for selected intervals during Transition 1 and each of the five quasi-stable patterns observed between June 2000 and June 2001. Pattern 1: August 13–September 30, 1999. Transition 1: November 11–December 31, 1999. Pattern 2: February 2–June 10, 2000. Pattern 3: June 17–November 5, 2000. Pattern 4: November 29, 2000–March 21, 2001. Pattern 5: April 16–June 21, 2001.

near 36°35′N, 131°35′E south of Dok Island. Its shape and position varied with fluctuations of the OB position, changing from circular when the OB was weak to slightly elliptical when it was strong.

From July 22 to August 16 a small cold-core eddy was observed northeast of Ulleung Island and persisted while propagating generally west. On August 21 it coalesced with the EKWC. During the eddy's transit, the loop current was suppressed north of Ulleung Island and the major axis shrank to about 200 km, and the EKWC temporarily separated perpendicular to the coast. After the eddy transited (August 31), the EKWC returned to its previous path, and warm water filled the region from east of the tip of the Oki Bank to the northern tip of the Ulleung Warm Eddy.

5.2. Transition 1: Warming Basin

The transition between Patterns 1 and 2 (October 1, 1999–February 1, 2000) progressed through three stages (Figs. 2 and 4). The first stage began when the water of the elliptical loop warmed and expanded to the northeast between October 1 and November 3. The second stage began when the Ulleung Warm Eddy moved north, almost tripled its size, and filled the entire northern portion of the Ulleung Basin from the confluence region of the EKWC/NKCC to the Oki Bank between November 4 and December 14. When this occurred, the bifurcation of the EKWC ceased and the loop current was incorporated into the Ulleung Warm Eddy. The Dok Cold Eddy maintained its position throughout the movement and expansion

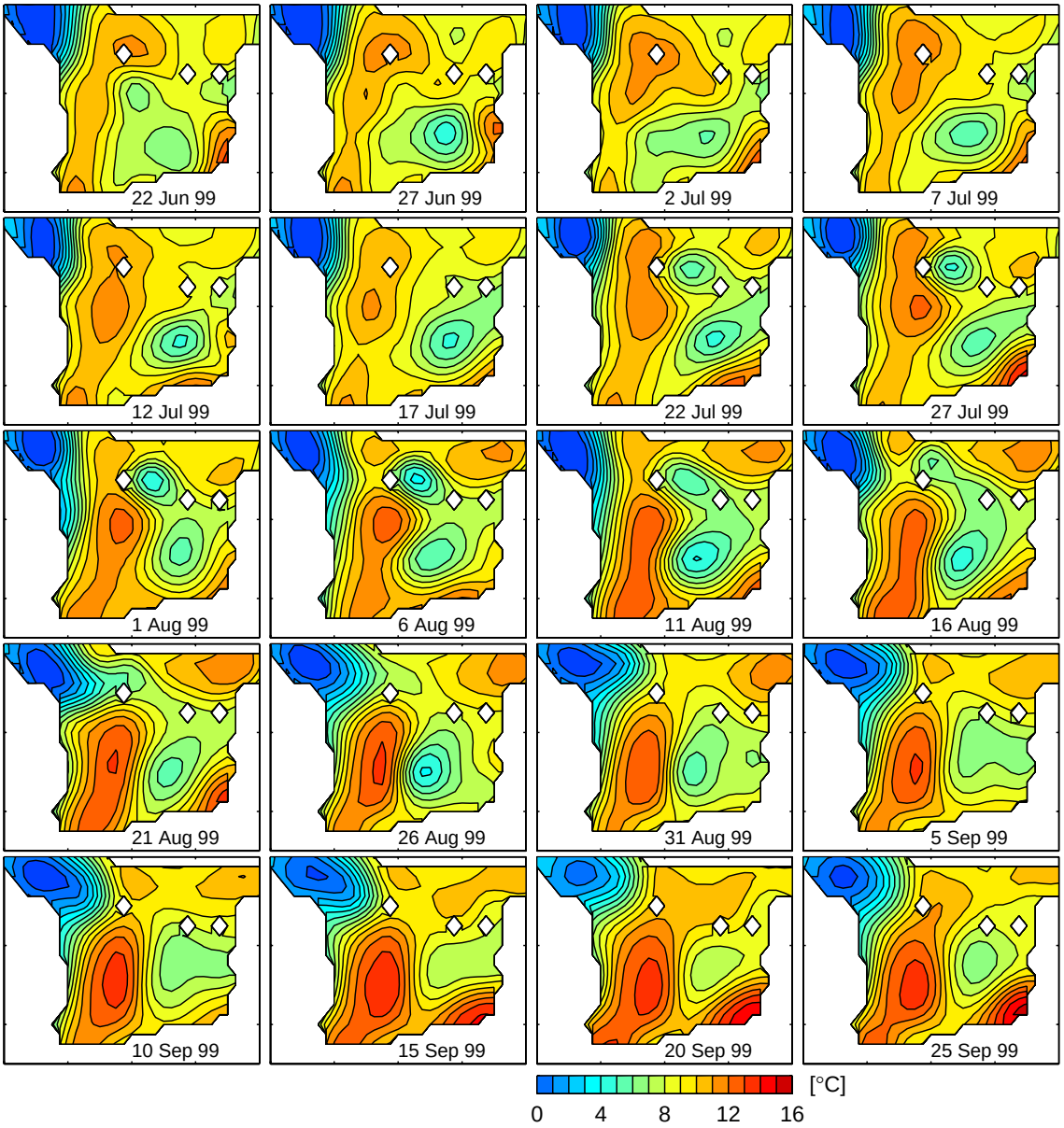

Fig. 3. Time series of Pattern 1 temperature at 100 dbar at 5-day intervals. Contour interval is 1 °C. The geographic region mapped is the same as in Fig. 2.

of the Ulleung Warm Eddy, although it did warm. The third stage began on December 15, when two processes occurred: (1) the EKWC bifurcated near 36°N, with one branch continuing north as the EKWC. The other branch flowed south and merged with the OB. During this period, the Dok Cold Eddy propagated westward towards the coast of Korea. (2) The Ulleung Warm Eddy began decreasing in size as cooler waters penetrated the Ulleung Basin from the northeast along 132°30′E, reaching as far south as Dok Island. The Ulleung Warm Eddy shrank in size until it was roughly circular in cross-section with a diameter of 125 km, centered on Ulleung Island.

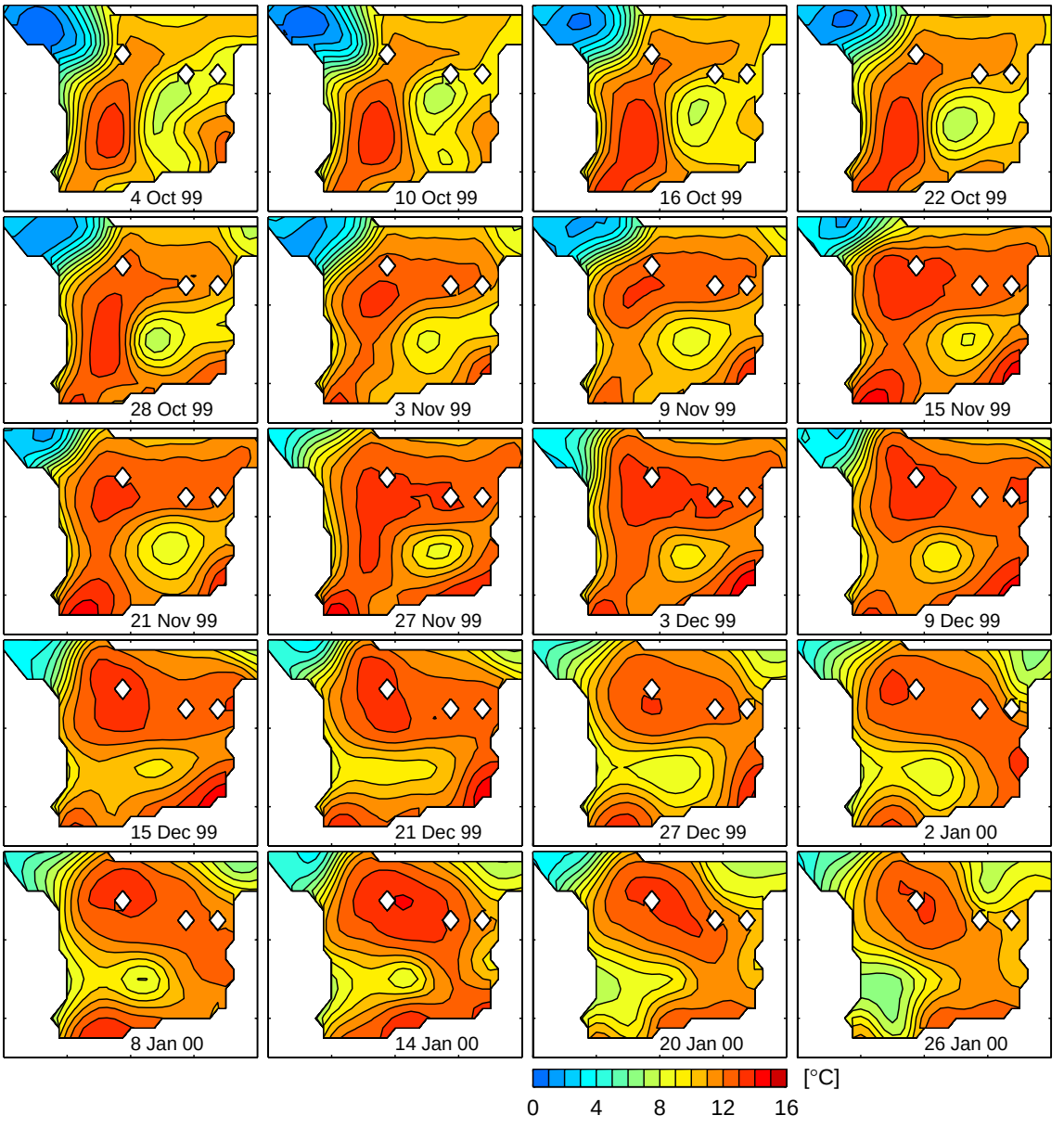

Fig. 4. Time series of Transition 1 temperature at 100 dbar at 6-day intervals. Contour interval is 1 °C. The geographic region mapped is the same as in Fig. 2.

5.3. Pattern 2: Ulleung Eddy/two branches

Pattern 2 (Figs. 2 and 5), observed from February 2 to June 10, 2000, had four major features. First, the Ulleung Warm Eddy maintained its size and position centered around and south of Ulleung Island throughout the pattern. Its shape constantly evolved with the movement of the Dok Cold Eddy, and with the southward intrusion of the Subpolar Front late in May.

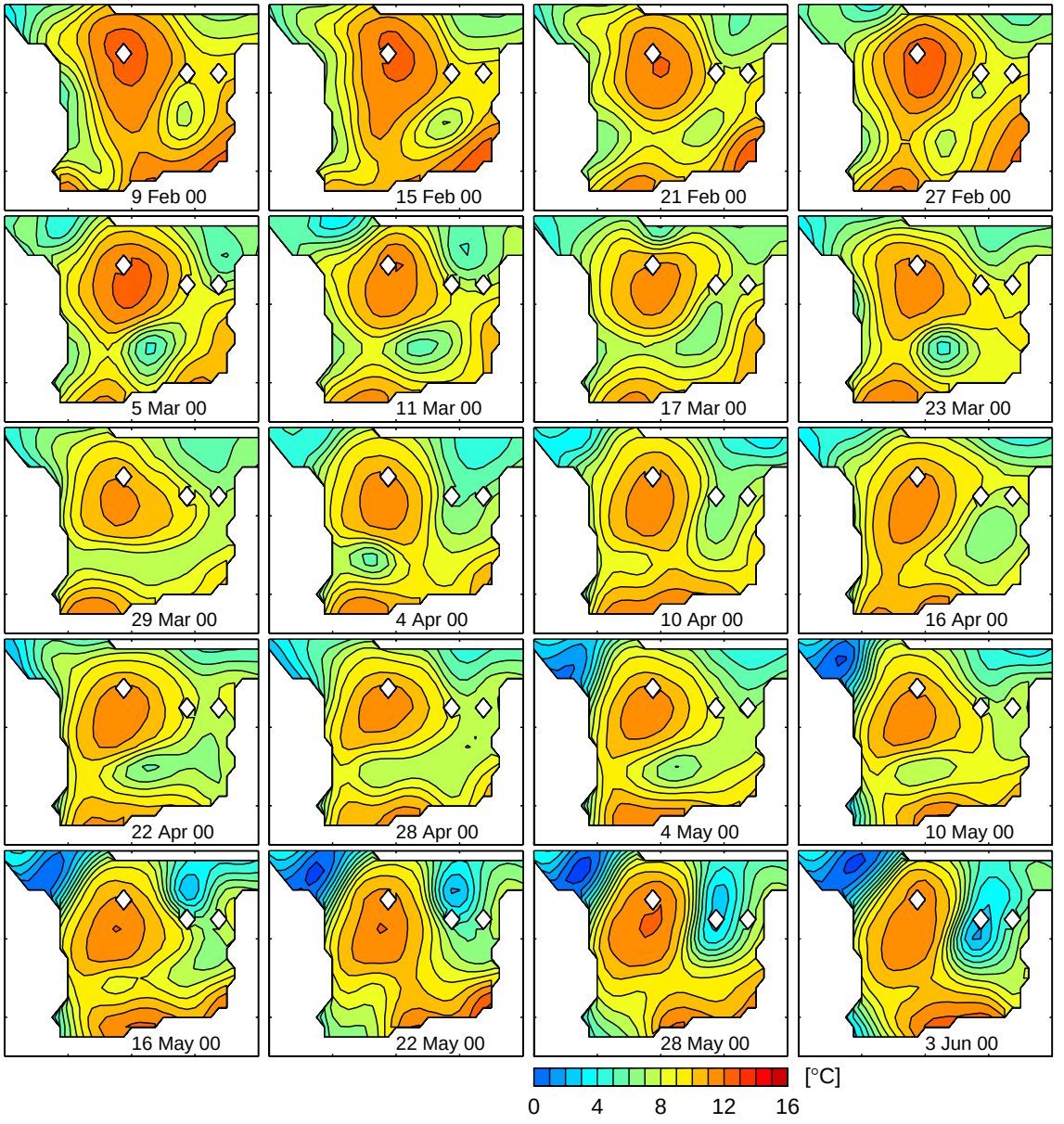

Fig. 5. Time series of Pattern 2 temperature at 100 dbar at 6-day intervals. Contour interval is 1 °C. The geographic region mapped is the same as in Fig. 2.

Second, the Dok Cold Eddy re-formed in February when a cold-core eddy was shed from the Subpolar Front east of the Ulleung Warm Eddy. It propagated westward south of Ulleung Island until it reached the coast of Korea on April 6. A second eddy formed on April 14, and immediately propagated westward and reached the coast of Korea on May 18. Third, the EKWC was affected by the propagation of the Dok Cold Eddy. The EKWC temporarily diverted eastward south of

36°15′N each time the Dok Cold Eddy approached the coast of Korea, but returned to its previous path after the eddy merged with the cool waters found there. Fourth, the OB was present throughout the pattern. It typically entered the Ulleung Basin near 130°30′E and flowed along the 1000 m isobath. Beginning on May 10, a meander trough of the Subpolar Front intruded southward between Ulleung and Dok Islands. By May 22 the trough had extended southward until its flow merged with the OB, giving the flow pattern the appearance of one large meander. However, the temperature of the OB remained about 2 °C warmer than the water brought southward along the meandering Subpolar Front.

5.4. Transition 2: EKWC disappearance

The transition between Patterns 2 and 3 occurred between June 11 and 16, 2000 when a meander trough of the Subpolar Front that began in Pattern 2 continued to grow in amplitude until it came into contact with cold waters extending eastward from the coast of Korea. The connection of the cold waters severed the path followed by the EKWC, diverting the warm inflow fully into the OB, strengthening it significantly. The Ulleung Warm Eddy became isolated and completely surrounded by cold waters.

5.5. Pattern 3: Small Ulleung Eddy/Cold Basin/EKWC absent

Pattern 3 (Figs. 2 and 6), which lasted from June 17 to November 5, 2000, was characterized by the absence of the EKWC, the steadiness of the OB, and the rapid shrinkage of the Ulleung Warm Eddy. Additionally, by early August, the mean position of the Subpolar Front had moved south to 37°30′N, and much of the Ulleung Basin was filled with cold water. On June 28, a streamer of warm water from the northeast side of the Ulleung Warm Eddy converged with the OB (near 37°30′N). This connection between the Ulleung Warm Eddy and OB lasted until August 7. During this period, the Ulleung Warm Eddy lost about half its volume, shrinking to a diameter of about 60 km. After the warm connection between the Ulleung Warm Eddy and OB was broken, the two features remained relatively stable in their positions and strengths. The Ulleung Warm Eddy remained centered on 37°N, 130°45′E, while the OB generally flowed along the 1000 m isobath and exited the Ulleung Basin along the northern tip of the Oki Bank.

5.6. Transition 3: Reestablishment of the EKWC/Dok Cold Eddy

Two events occurred during the transition between Patterns 3 and 4 (November 6 and 28, 2000). First, the eastward flowing OB developed a northward meander at 130°30′E that made contact with the Ulleung Warm Eddy, severing the cold-water connection between the Subpolar Front and the cold water along the coast of Korea. This event appears to have reestablished the EKWC. Second, the Subpolar Front shed a Dok Cold Eddy and then retreated northward to 37°30′N, flowing along an easterly path.

5.7. Pattern 4: Ulleung Eddy/two branches/weak Subpolar Front intrusion

Pattern 4 (November 29, 2000–March 21, 2001) was similar to Pattern 2 with several key differences (Figs. 2 and 7). (1) the diameter of the Ulleung Warm Eddy was approximately half as large as in Pattern 2, and it was centered about 50 km farther to the west, near 37°15′N, 130°20′E. The Ulleung Warm Eddy cooled about 3 °C over the course of the pattern. (2) The Subpolar Front shifted southward to a meandering path across the northern Ulleung Basin. (3) The Dok Cold Eddy was larger and did not propagate toward the coast of Korea. However, the Subpolar Front twice developed steep troughs that temporarily enveloped the Dok Cold Eddy. After the first envelopment (January 29, 2001), the Subpolar Front retreated northward, re-forming the Dok Cold Eddy as a distinct feature again. In contrast, the second steep trough remained (March 12, 2000) and the Dok Cold Eddy was no longer distinguishable. (4) The OB extended farther to the north along the Oki Bank, reaching 37°30′N, and it was about 2 °C cooler.

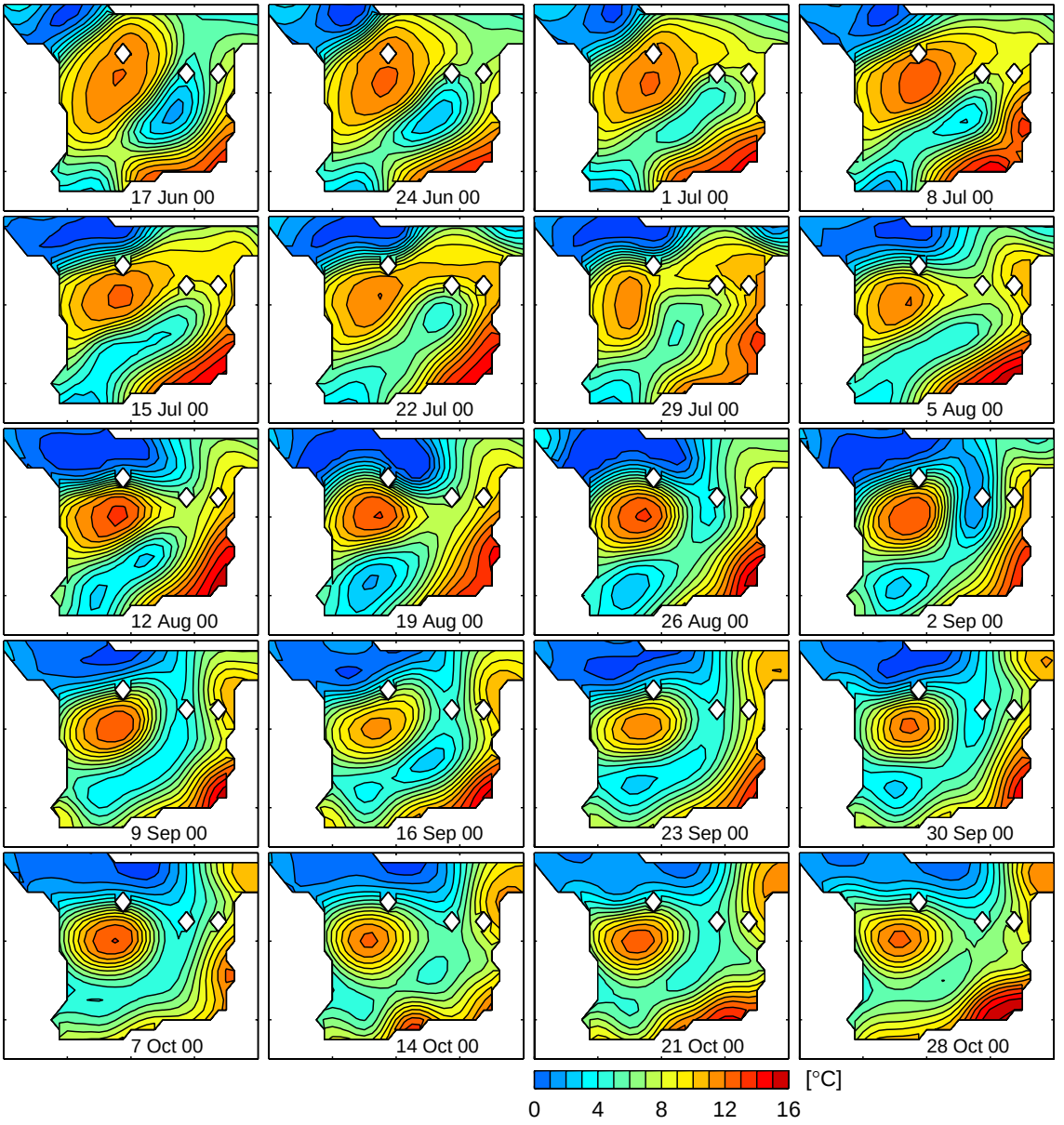

Fig. 6. Time series of Pattern 3 temperature at 100 dbar at 7-day intervals. Contour interval is 1 °C. The geographic region mapped is the same as in Fig. 2.

5.8. *Transition 4: Strengthening EKWC*

Transition 4 occurred from April 9 to 15, 2001 when the Ulleung Warm Eddy narrowed and elongated to the southwest. During this lengthening process, the Ulleung Warm Eddy lost its identity and became an elongated loop of current similar to Pattern 1. The loop of current came into contact and merged with the OB, forming one large meander.

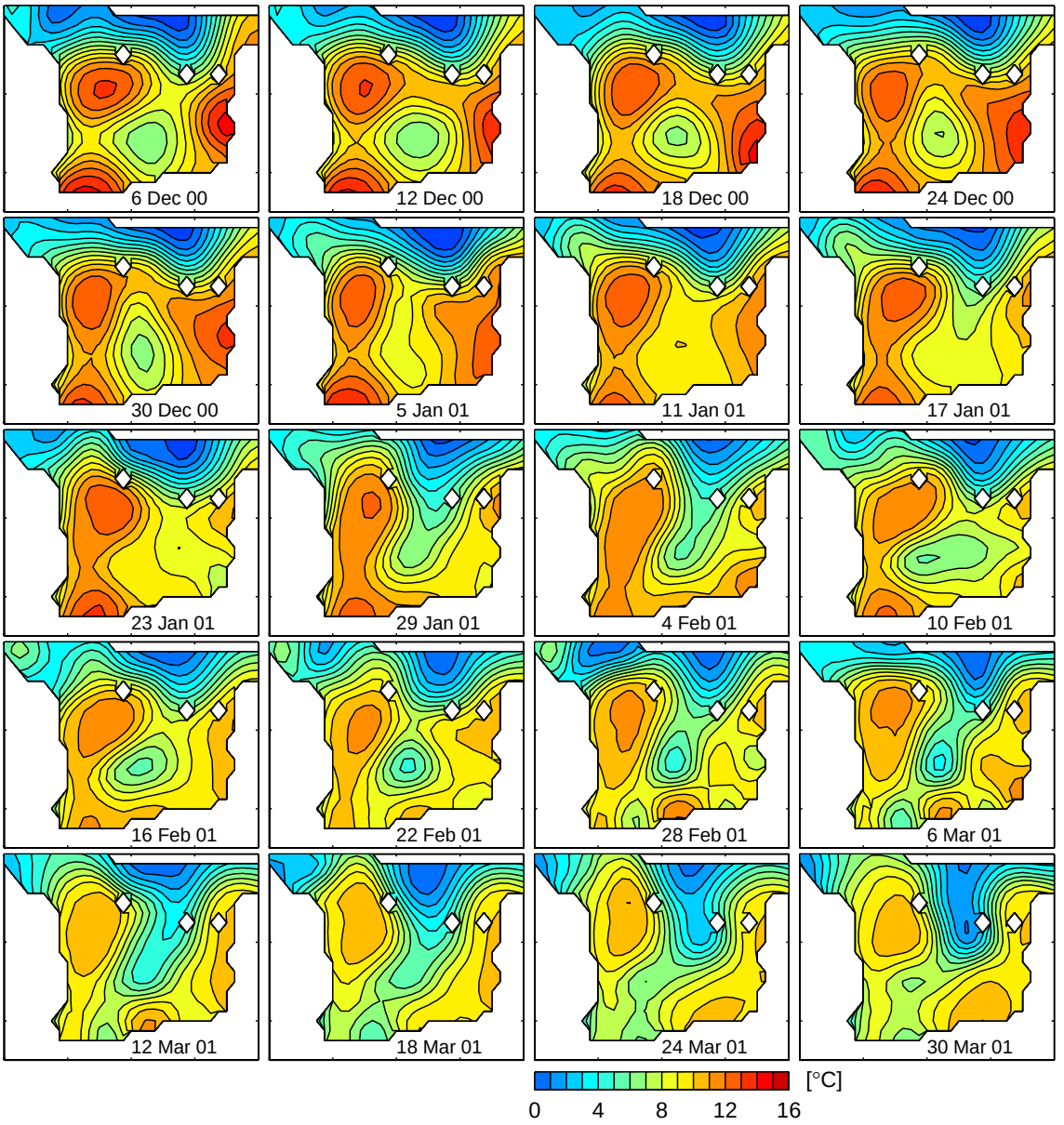

Fig. 7. Time series of Pattern 4 temperature at 100 dbar at 6-day intervals. Contour interval is 1 °C. The geographic region mapped is the same as in Fig. 2.

5.9. *Pattern 5: Large meander/strong Subpolar Front intrusion*

Pattern 5 (April 16–June 21, 2001, when the array was recovered) was dominated by the warm loop of current, the OB, and a large meander trough of the Subpolar Front (Figs. 2 and 8). The warm loop of current was confined on its west side by the EKWC, which was located inshore of the 1000 m isobath (inshore of our array), and separated from the coast of Korea near 38°N. The warm loop was confined on its east side by a

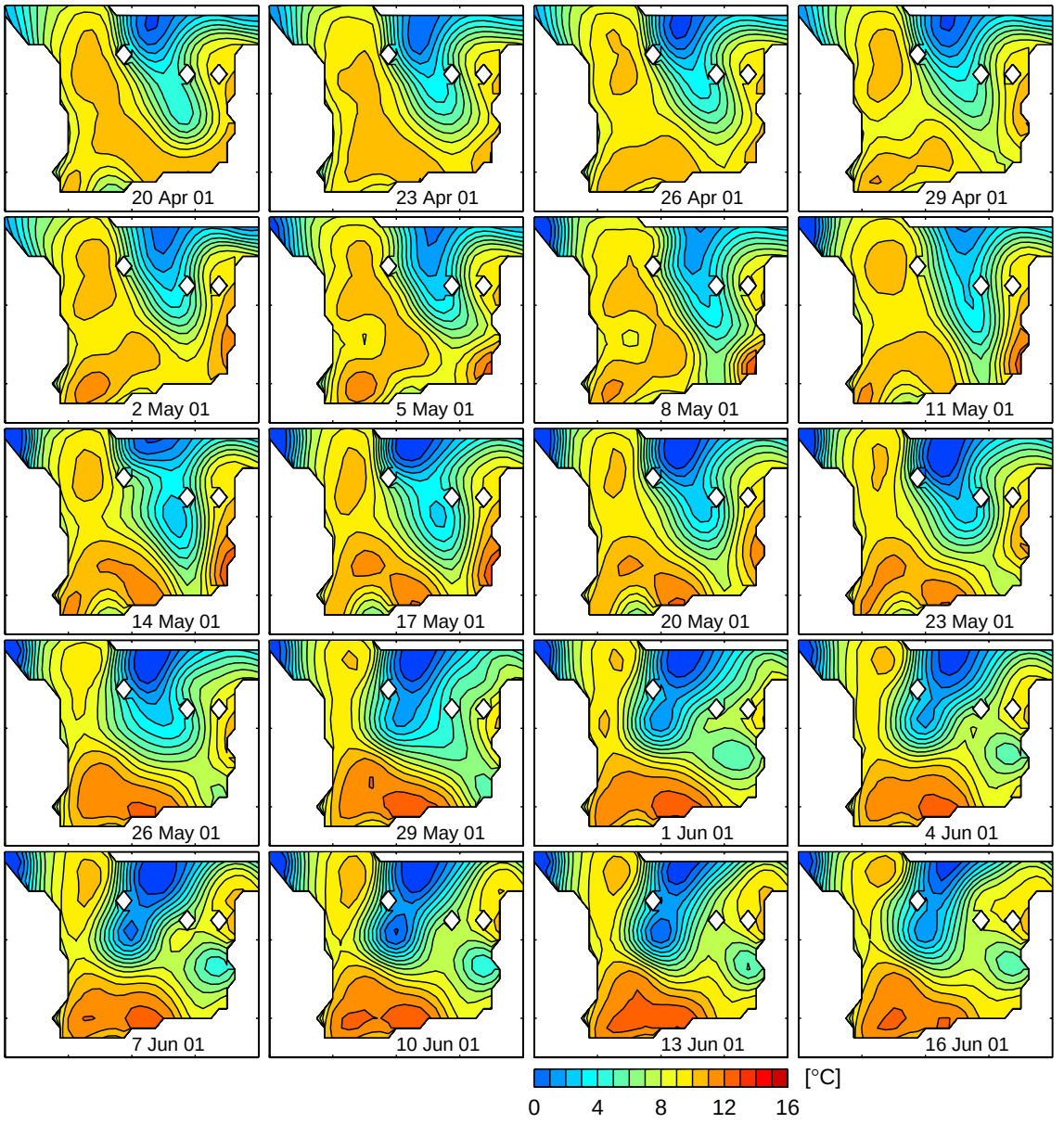

Fig. 8. Time series of Pattern 5 temperature at 100 dbar at 3-day intervals. Contour interval is 1 °C. The geographic region mapped is the same as in Fig. 2.

meander trough of the Subpolar Front, which brought cold water into the basin between Ulleung and Dok Islands as far south as 36 °N. On May 14, the OB developed a warm northward meander centered near 130°E that reached 36°30′N. On May 29 two events occurred when the Subpolar Front meander trough shed a Dok Cold Eddy: (1) The orientation of the meander trough and the warm loop changed from northwest/southeast to north/south, and (2) the OB developed a westward meander along the Oki Bank near 37°N that extended slightly west of Dok Island.

6. Verification

The Residual GEM Technique works most reliably when there is a nearly unique relationship between acoustic travel time and the vertical structure in the region being investigated. It is possible (and does occur) that different T and δ profiles produce the same travel-time values, and correspondingly the Residual GEM Technique estimated $T(p)$ and $\delta(p)$ values have errors. In the southwestern JES the Residual GEM Technique estimates account for more than 89% of the T variance and 84% of the δ variance contained in the historical data (Mitchell et al., 2004). Further verification of the Residual GEM Technique, during the period the PIES were deployed, is accomplished through comparisons with independently collected data.

Fig. 9 displays four comparisons (February, April, June, and October 2000) with National Fisheries Research and Development Institute of Korea CTD data (provided by KORDI). Temperature at 100 dbar is contoured. The Korean CTD data were collected along six repeat lines in the Ulleung Basin, eastward from the Korean coast to 131°30′E. The PIES locations were chosen to be close to these lines in the north/south direction, but the CTD station spacing was finer in the east/west direction, with station spacing expanding from about 10 km adjacent to the coast to about 25 km offshore. The rms difference between the PIES derived maps and the CTD measured maps is 1.5 °C. However, the CTD maps, due to the higher resolution of the CTD measurements, clearly capture small scale features that the PIES measurements do not. The right column of Fig. 9 shows maps constructed from a subsampling of the CTD data onto the PIES sites. The rms difference between these maps and the PIES derived maps is reduced to 0.94 °C, illustrating the effects of small scale features on the error between the PIES and CTD measured maps. For each case, the mesoscale features mapped by the PIES array are verified by the maps from the CTD sections, and in each case the CTD data resolve additional smaller-scale features. In particular, the PIES maps correctly determined several important mesoscale features: the absence or presence of the EKWC and its path and separation latitude; the size, position, and variability of the Ulleung Warm Eddy; and the path of the Subpolar Front when it passed through the Ulleung Basin during late 2000 and 2001 (not shown).

Fig. 10 shows the temperature mapped by the PIES array at 50, 100, and 150 dbar time-averaged over the period 24 June–2 July, 1999. Fig. 8 (panels b,d, and e) of Ramp et al. (2005) shows a composite map of "pseudo-profiles" taken over the same period, also at 50, 100, and 150 dbar. The "pseudo-profiles" are a combination of deep CTD casts and CTD data collected with a towed Video Plankton recorder (VPR) to a depth of about 80 m, combined using a different GEM technique. Their CTD casts and VPR data were collected along lines that coincided with the PIES lines in the north/south direction. The resolution in the east/west was finer than the PIES, with the "pseudo-profiles" having 3.5-km resolution. A comparison of these two figures further demonstrates the ability of the Residual GEM Technique's ability to capture mesoscale features at various depths with good temperature resolution. (Fig. 11)

The differences between maps produced using the Residual GEM interpreted PIES data and maps produced from other methods can be mainly attributed to resolution differences in the data collection. For example, small scale features are present in the Korean CTD data along the southern edge of the Ulleung Basin, and along the coast of Korea in shallow water outside the PIES array. However, when the CTD data is subsampled to the PIES locations, the rms difference is reduced from 1.5 to 0.94 °C, which is within the expected error limits of the Residual GEM Technique (~1.25 °C) at 100 dbar. Features of similar scale are also present in Fig. 8, panel b of Ramp et al. (2005), which shows two small warm eddies, one centered near 37°30′N, 130°45′E, and the other near 36°30′N, 130°15′E. These features occur between PIES locations and are smaller than the PIES separation distance. In cases such as these, the features were unmeasured, and not mapped by the PIES data. Thus, it is the station spacing of the PIES array that made it unsuitable for resolving features on scales smaller than 50 km that occur between PIES measurement sites, not

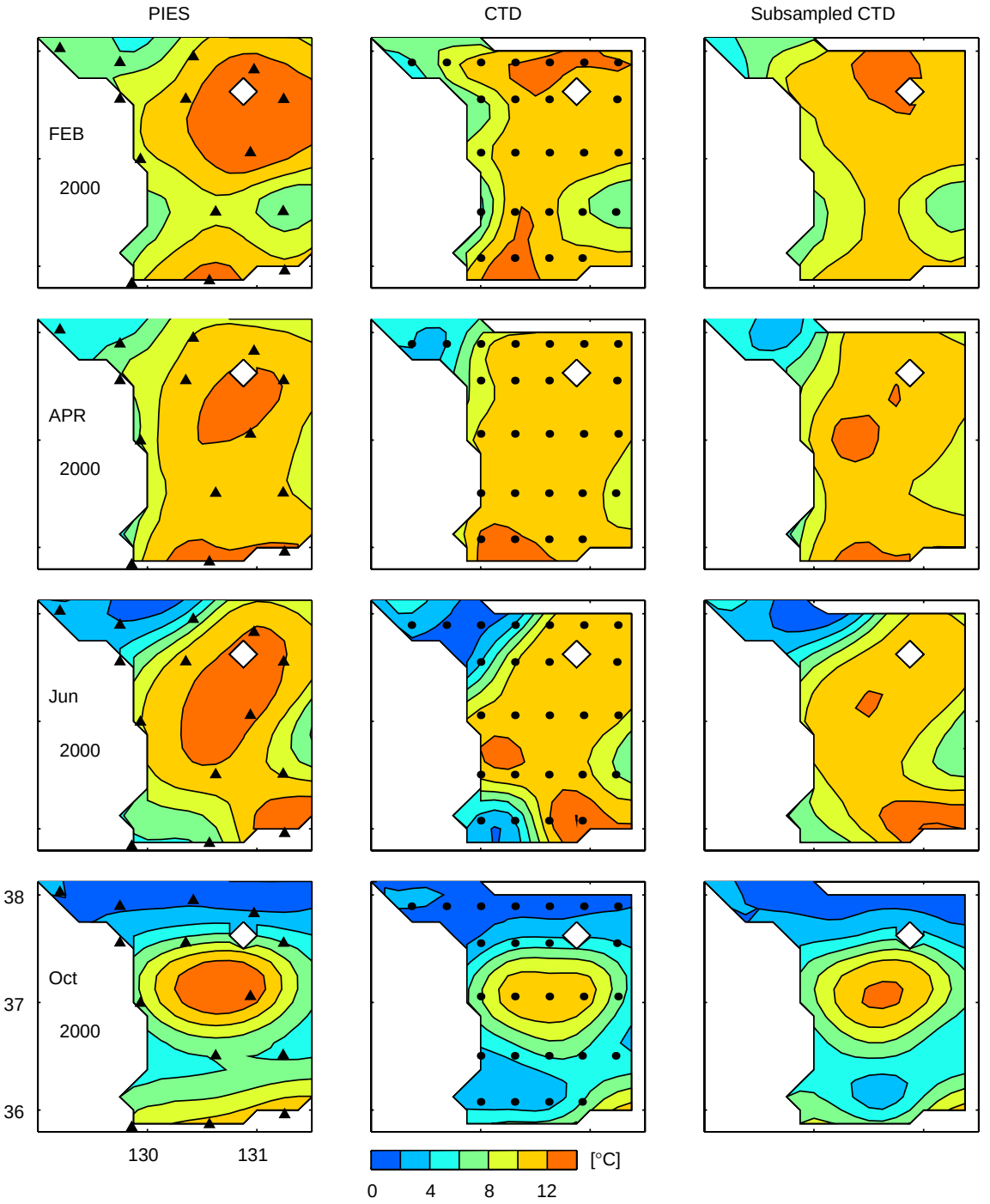

Fig. 9. Optimally interpolated maps of temperature at 100 dbar generated from PIES data interpreted with the Residual GEM Technique (left column) and generated from Korean CTD data (center column) in February, April, June, and October 2000. The PIES data were averaged over the duration of the CTD collection period. Contour interval is 2 °C. PIES locations are marked by black triangles and CTD locations by black dots. Right column: CTD data subsampled to PIES locations.

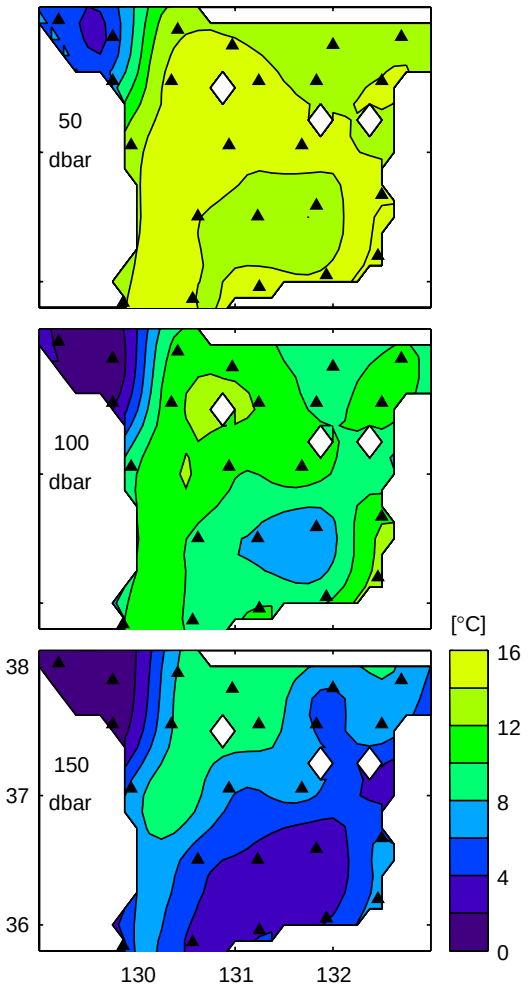

Fig. 10. Average temperature at 50, 100, 150 dbar between June 24 and July 2, 1999 for comparison with Fig. 8b, d, and e of Ramp et al. (2005). Contour interval is 2 °C.

inadequacies of the Residual GEM Technique. Additional differences arise because these other methods are not synoptic, while the PIES data are synoptic. The first three panels of Fig. 3 (22 June–2 July, 1999) display the temporal evolution of the temperature at 100 dbar during the period depicted in Fig. 8 panel d of Ramp et al. (2005); they clearly show changes occurred during the CTD data collection survey. The advantages of the PIES data are the high temporal resolution, and the ability to collect truly synoptic data continuously for extended periods of time. Hence, with the PIES

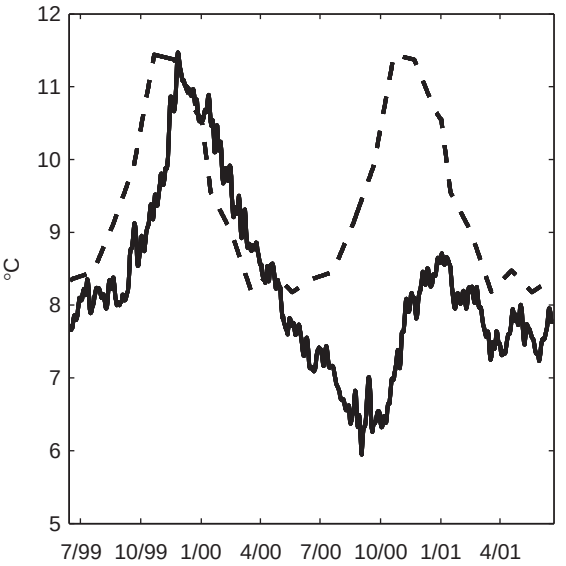

Fig. 11. Daily mean temperature in the Ulleung Basin at 100 dbar measured by the PIES array (as shown in Figs. 3–8) (solid line). Climatological mean Ulleung Basin temperature at 100 dbar from MODAS (dashed line).

data, we can analyze the short-term tendencies and (unaliased) long-term evolution of the whole current system.

7. Circulation pattern features

At least five persistent non-repeating current patterns were identified in the Ulleung Basin between June 1999 and July 2001 (Fig. 2). Transition 1 (between Patterns 1 and 2) lasts four months. Transitions 2–4 each occur in three weeks or less. Patterns 1, 2, and Transition 1 occur during Year 1 when the Ulleung Basin is warmer than the three remaining patterns, in Year 2. Pattern 3 is markedly different than the other four patterns due to the absence of the EKWC, the strength and steadiness of the OB, and the circulation of cold water in a closed circuit surrounding the Ulleung Warm Eddy.

The "three branch" paradigm first introduced by Suda and Hidaka (1932) and Uda (1934) and the single meander view presented by Moriyasu (1972), while attractive for their simplicity, both require updating based on our findings. The

time-series of synoptically mapped temperature fields for the entire Ulleung Basin presented here highlights the complicated temporal evolution of the Ulleung Basin current pattern, which does not fit into the "three branch/single meander" descriptions traditionally adopted. For example, Pattern 5 (Fig. 2) resembles the single meander description of Moriyasu; however, closer examination reveals that the EKWC branches both north and south of 36°N. In addition, mesoscale variability plays a significant role in the current patterns (Figs. 3–8), highlighting the importance of synoptic measurements. The maps of temperature at 100 dbar suggest five features may be used to describe the basic current pattern in the Ulleung Basin: the OB, EKWC, Ulleung Warm Eddy, Dok Cold Eddy, and the Subpolar Front. These five features, based on their presence or absence, size, position, and orientation (separation angle and latitude of EKWC, path of Subpolar Front), contain the basic information required to deduce the basic current pattern in the Ulleung Basin. However, care must be taken when interpreting non-synoptic measurements due to the vigorous mesoscale variability that appears to be continuously present in the Ulleung Basin.

7.1. Offshore Branch

The OB was present during each season of this 2-year measurement period (Figs. 3–8). From June 15 to August 1, 1999, the water in the OB was several degrees warmer than the water in the EKWC, suggesting it formed by branching of the Tsushima Warm Current south of our array in the Korea/Tsushima Strait. On August 1, the OB merged with the warm loop of current near 36 °N, 130°30′E into one large meander. When the Ulleung Warm Eddy formed later on August 26 the OB temporarily vanished from our measurement region, returning on September 10. During Transition 1 the OB was continuously present and its position constantly evolved in association with movement of the Dok Cold Eddy. The OB was highly variable during Pattern 2, when the Dok Cold Eddy propagated toward Korea and merged with the cooler waters there on two separate occasions, diverting differing amounts of water into the EKWC and the OB. On May 22, a meander trough of the Subpolar Front that had extended southward between Ulleung and Dok Islands, merged with the OB into one large meander. However, the temperature of the OB remained about 2 °C warmer than Subpolar Front water, indicating branching still occurred upstream of the Ulleung Basin. During Pattern 3, the strength of the temperature gradient remained steady, but the OB path changed. The OB flowed eastward along the southern boundary until June 17, after which its path diverted northward along the Oki Bank, where it stayed for the remainder of Pattern 3. With reestablishment of the EKWC during Pattern 4, the OB currents were weaker and meandered more. The meanders consisted of a southward excursion near 36°N, 130°30′E, and a westward excursion near 37°15′N, 131°30′E that reached the Ulleung Warm Eddy. During Pattern 5 the warm loop of current re-formed and to its east the Subpolar Front penetrated far southward in a trough within the Ulleung Basin. As a result, a compound meander crest existed after 26 May, in which the warmest waters of the OB formed a small loop (to 36°30′N) inside the steeper loop (to north of 38°35′N).

7.2. East Korean Warm Current

The EKWC was absent from June 11 to November 5, 2000 when none of the warm water advected through the strait appeared to be transported north along the coast of Korea (Figs. 2 and 6). Absence of the EKWC was first reported by Kim and Legeckis (1986). Based on PIES data alone there existed the possibility that warm water flowed northward along the Korean shelf inshore of the PIES array. Nevertheless, the Korean CTD data confirmed its absence during June, August, and October, 2000. Interestingly, the disappearance and reestablishment of the EKWC was not directly linked to variations in total transport through the Korea/Tsushima Strait (V_{KTS}), but may have been associated with repeated westward propagation and subsequent merging of the Dok Cold Eddy with the EKWC. The EKWC vanished during Transition 2, and since the V_{KTS} must have diverted elsewhere, we infer that it must go into the

Nearshore and Offshore Branches to flow east along the coast and shelf break of Japan.

7.3. Ulleung Warm Eddy

The size and location of the Ulleung Warm Eddy (Figs. 2–8), which was present for 20 consecutive months from August 1999 until April 2001, appears to be affected by the northward transport of warm water by the EKWC. It initially formed in response to a rapid increase in V_{KTS} followed by a rapid decrease (Kim et al., 2004). The increase brought a tongue of warmer water into the Ulleung Basin that formed into a loop of current. The decrease isolated the loop current amidst cooler water where it formed into a compact warm-core eddy. During Transition 1 when the V_{KTS} reached its maximum during the experiment, the Ulleung Warm Eddy expanded in area by nearly a factor of three and filled the northern Ulleung Basin from west of Ulleung Island to east of Dok Island. As V_{KTS} steadily decreased from November 1999 to February 2000 the Ulleung Warm Eddy steadily decreased in size until it was approximately 100 km in diameter. It maintained this size and position for four months until mid-June 2000, at which time it diminished in size to a diameter of 60 km, and the temperature gradient along its southern edge decreased. The Ulleung Warm Eddy persisted in this configuration until April 2001, when it coalesced with a northward-advancing meander crest to form a steep warm loop of current, after which the Ulleung Warm Eddy ceased to exist as a separate feature.

7.4. Dok Cold Eddy

The Dok Cold Eddy was a highly variable, recurrent feature usually found southwest of Dok Island. It was generally smaller than the Ulleung Warm Eddy, with a mean diameter of 60–80 km, and a core temperature that ranged from 5 to 10 °C, and typically formed when the Subpolar Front looped southward between Ulleung and Dok Islands and shed an eddy. On several occasions it propagated westward and merged with the cold water along the coast of Korea. During the first two events, the EKWC deflected eastward until the Dok Cold Eddy had passed, and after the third event the EKWC ceased flowing northward. The EKWC and the Dok Cold Eddy were both absent between June and November 2000, when cold water completely encircled the Ulleung Warm Eddy. Although we name it as a new feature here, in retrospect evidence of it exists in earlier literature (Katoh, 1994, Fig. 8; Lie et al., 1995, Fig. 3a; Preller and Hogan, 1998, Fig. 15.23).

7.5. Subpolar Front

The position and orientation of the Subpolar Front were highly variable (Figs. 2–8) throughout our 2-year measurement period. From June 15, 1999 to June 10, 2000 (Patterns 1, T1, and 2) the mean position of the front was north of the Ulleung Basin and outside our PIES array. However, on several occasions, the front meandered southward between Ulleung and Dok Islands and subsequently shed a Dok Cold Eddy. Throughout this period the separation angle of the EKWC relative to the coast of Korea varied between 0° and 45° with a mean angle of 30°. From June 17, 2000 until June 21, 2001 (Patterns 3–5) the mean position of the Subpolar Front shifted southward into the Ulleung Basin. From June 16, 2000 until March, 8 2001, the separation angle of the EKWC remained near 90°. On March 12, 2001, the separation angle changed to approximately 0°, and a large meander of the front penetrated between Ulleung and Dok Islands, reaching as far south as 36°N. The meander persisted at least until June 16, 2001, when our instruments were recovered, and perhaps longer.

8. Circulation patterns in relation to Korea/Tsushima Strait transport and seasonal cycle

The mean temperature in the Ulleung Basin exhibited a seasonal signal that appears to be modulated by V_{KTS}. The transport measurements were taken using a cable that crosses from Korea to Japan slightly north of Tsushima Island (Kim et al., 2004). The seasonal signal in the Ulleung

Basin at 100 dbar was characterized by a temperature rise in late summer/early fall followed by a gradual cooling throughout winter and spring. This signal is readily apparent (Kim et al., 2004), but shifted by about one month later than climatological values. It was clearly stronger in Year 1 than Year 2. This change in strength and shift in time of the seasonal variation probably result from the mean V_{KTS} being higher in fall/winter 1999–2000 (3.12 Sverdrups (Sv)) than either the fall/winter 2000–2001 (2.35 Sv), or summer 1999. In the Fall of Year 1, while the waters advecting through the Korea/Tsushima Strait are climatologically warmest, V_{KTS} reached its peak value during our measurement period, 4.2 Sv. The EKWC presented an efficient conduit to fill the Ulleung Basin with warm waters during that period. In contrast, during the succeeding ten months (01/00–10/00), after the V_{KTS} fell to exceptionally low values, the temperatures of the upper Ulleung Basin fell steadily, even through the next summer months when according to climatology they normally would have warmed. The EKWC was clearly absent (Pattern 3) during June–November 2000. As a result, the warm water the EKWC normally would have transported into the Ulleung Basin were presumably transported elsewhere, the Nearshore and Offshore Branches along the southern edge of the basin. The warming did eventually occur about four months late in a two-month event during October and November 2000, but in the next six months the temperatures remained below climatological average values.

The patterns in Year 1 appear to be associated with V_{KTS} changes, while the patterns in Year 2 do not. The warming in Pattern 1 is matched by an increase in V_{KTS} (Kim et al., 2004). Transition 1 begins when the V_{KTS} reaches its maximum value of 4.2 Sv in October 1999. Following this peak, the Ulleung Warm Eddy greatly expands in size as the Ulleung Basin with fills with warm water. The V_{KTS} decreases from this maximum to its minimum value of 1.4 Sv at the end of January, 2000, during which time the Ulleung Basin steadily cools and the Ulleung Warm Eddy shrinks. Pattern 2 starts with an increase in V_{KTS} to approximately 2.4 Sv in mid-March, 2000. Transitions 2–4, and Patterns 3 and 4 are not accompanied by V_{KTS} variations. In fact, V_{KTS} is remarkably small and steady and the variation is reduced from mid-March 2000 to June 2001.

9. Conclusions

When interpreted with the Residual GEM Technique, the PIES data collected between June 1999 and July 2001 illustrate the complicated circulation patterns and intense mesoscale eddy activity in the Ulleung Basin. During this period the Ulleung Basin displayed at least five persistent current patterns with strong inter-seasonal variability and no clear seasonal signal below the mixed layer. A new framework for describing the current patterns in the Ulleung Basin based on particular attributes of the EKWC, Ulleung Warm Eddy, OB, Dok Cold Eddy, and the Subpolar Front at 100 dbar depth is presented.

The size and position of the Ulleung Warm Eddy is sensitive to V_{KTS} and the northward transport of warm water via the EKWC. The Ulleung Warm Eddy formed in August 1999 while V_{KTS} was increasing, and persisted for 20 months. In October 1999, when V_{KTS} reached its peak of 4.2 Sv, the Ulleung Warm Eddy increased in area until it filled the entire northern Ulleung Basin. When the V_{KTS} decreased from November 1999 to January 2000, the Ulleung Warm Eddy steadily decreased its area, and stabilized when the V_{KTS} stabilized. From June 17 through November 5, 2000 (Pattern 3), when the EKWC was absent, the Ulleung Warm Eddy decreased its diameter by a factor of two during the first month and then persisted for the next four months. From November 29, 2000 through March 21, 2001 (Pattern 4) the EKWC weakly reestablished itself and the area of the Ulleung Warm Eddy grew slightly in size. From March 12 through June 21, 2001 (Patterns 4 and 5) a strong meander trough of the Subpolar Front brought the cold front strongly southward in the eastern Ulleung Basin to about 36°N, and a steep narrow meander occupied the location of the former Ulleung Warm Eddy.

The position of the Subpolar Front in the Ulleung Basin appears to be influenced by V_{KTS}. V_{KTS} ranged from 3 to 4.2 Sv (i.e. exceptionally

high) in 1999 when the Subpolar Front remained north of the Ulleung Basin. However, in January 2000 V_{KTS} fell below 1.8 Sv (exceptionally low for the next four months), and the Subpolar Front moved southward to separate from the boundary at about 37°30′N, and eventually meandered southward between Ulleung and Dok Islands with a trough reaching as far south as 36°N. The V_{KTS} remained low (2 Sv) from April 2000 to April 2001 and a sequence of events occurred: absence of the EKWC, shrinking of the Ulleung Warm Eddy, southward meander of the Subpolar Front engulfing the Dok Cold Eddy—all associated with a generally cooler Ulleung Basin.

The OB is highly variable, present almost continuously during the two-year measurement period, and progresses through several stages. These stages include: (1) branching south of the Ulleung Basin in the Korea/Tsushima Strait, as indicated by the OB being several degrees warmer than the EKWC; (2) high variability in position and strength when the Dok Cold Eddy propagates westward towards Korea and diverts differing amounts of water into the EKWC and OB; (3) strengthening and changing path from east along the southern shelf break to north along the Oki Bank during the absence of the EKWC in Pattern 3; (4) high variability and meandering after the reestablishment of the EKWC in Pattern 4 until the end of the measurement period; and (5) during Pattern 5 the Subpolar Front meandered southward until it merged with the OB, giving the impression of one large meander. However, the OB was warmer than the meandering Subpolar Front, indicating the OB still formed through branching of the Tsushima Warm Current in the Korea/Tsushima Strait, and not by branching of the EKWC or meandering of the Subpolar Front.

The Dok Cold Eddy, though highly variable in space and time, is a recurrent and persistent feature generally located southwest of Dok Island. Its movement from this general position is associated with the position of the Subpolar Front. When the Subpolar Front meanders southward between Ulleung and Dok Islands it either forces the Dok Cold Eddy to propagate westward until it merges with the cold waters near the coast of Korea, or it merges with the Dok Cold Eddy and incorporates it into the meander. However, when the meander retreats, another Dok Cold Eddy is subsequently shed again. The Dok Cold Eddy is completely absent only during Pattern 3, when instead cold waters fill a large meander trough in the eastern Ulleung Basin.

Acknowledgements

This work was supported by the Office of Naval Research "Japan/East Sea DRI". Basic Research Programs include the Japan/East Sea initiative under grant N000149810246 and the Naval Research Laboratory's "Linkages of Asian Marginal Seas" under Program Element 0601153N. M.-S. Suk and K.-I. Chang were supported by grants from KORDI's in-house projects (PE82500 and PE83300). J.-H. Yoon was supported by a grant from the Japan Marine Science Foundation under program "Study of intermediate and deep circulation of the Japan Sea". The authors would also like to thank the officers and crews of the R/V ROGER REVELLE during cruise Hahnaro VI, and the R/V MELVILLE during cruise Cook Leg 9 for their skill and dedication during the deployment and recovery of the instruments. The CTD data were kindly provided by the Korea Oceanographic Data Center.

References

An, H.S., Shim, K.-S., Shim, H.-R., 1994. On the warm eddies in the southwestern part of the East Sea (the Japan Sea). Journal of the Oceanological Society of Korea 29, 152–163.

Chang, K.-I., Hogg, N.G., Suk, M.-S., Byun, S.-K., Kim, Y.-G., Kim, K., 2002. Mean flow and variability in the southwestern East Sea. Deep-Sea Research I 49, 2261–2279.

Cho, K.-D., Bang, T.-J., Shim, T.-B., Yu, H.-S., 1990. Three dimensional structure of Ullung Warm Lens. Bulletin of the Korean Fisheries Society 23, 323–333.

Fox, D.N., Teague, W.J., Barron, C.N., Carnes, M.R., Lee, C.M., 2002. The Modular Ocean Data Assimilation System (MODAS). Journal of Atmospheric and Oceanic Technology 2, 240–252.

Hideaki, H.J., Yoon, H., Wataru, K., 1999. The path of the Tsushima Current along the Japanese cost. Journal of Oceanography 55, 217–235.

Ichiye, T., Takano, K., 1988. Mesoscale eddies in the Sea of Japan. La Mer 26, 69–79.

Isoda, Y., Saitoh, S.-I., 1993. The northward intruding eddy along the east coast of Korea. Journal of Oceanography 49, 443–458.

Katoh, O., 1994. Structure of the Tsushima Current in the southwestern Japan Sea. Journal of Oceanography 50, 317–338.

Kawabe, M., 1982a. Branching of the Tsushima Current in the Japan Sea. I. Data analysis. Journal of the Oceanographical Society of Japan 38, 95–107.

Kawabe, M., 1982b. Branching of the Tsushima Current in the Japan Sea, Part II. Numerical Experiment. Journal of the Oceanographical Society of Japan 38, 183–192.

Kim, K., Legeckis, R., 1986. Branching of the Tsushima Current in 1981–1983. Progress in Oceanography 17, 265–276.

Kim, K., Kim, K.-R., Chung, J., Yoo, H., Park, S., 1991. Characteristics of physical properties in the Ulleung Basin. Journal of the Oceanographical Society of Japan 26, 83–100.

Kim, K., Lyu, S.J., Kim, Y.-G., Choi, B.H., Taira, K., Perkins, H.T., Teague, W.J., Book, J.W., 2004. Monitoring volume transport through measurement of cable voltage across the Korea Strait. Journal of Atmospheric and Oceanic Technology, 21, 671–682.

Lie, H.-J., Byun, S.-K., Bang, I., Cho, C.-H., 1995. Physical structure of eddies in the southwestern East Sea. Journal of the Korean Society of Oceanography 30, 170–183.

Matsuyama, M., Kurita, Y., Senjyu, T., Koike, Y., Hayashi, T., 1990. The warm eddy observed east of Oki Islands in the Japan Sea. Umi to Sora 66, 67–75.

Meinen, C.S., Watts, D.R., 2000. Vertical structure and transport on a transect across the North Atlantic Current near 42 degrees N: timeseries and mean. Journal of Geophysical Research 105, 21869–21891.

Mitchell, D.A., Wimbush, M., Watts, D.R., Teague, W.J., 2004. The Residual GEM Technique and its application to the Southwestern Japan/East Sea. Journal of Atmospheric and Oceanic Technology, 21, 1895–1909.

Miyao, T., 1994. The fractal dimension analysis applied to eddies in the Sea of Japan. The Oceanographical Magazine 44, 13–30.

Morimoto, A., Yanagi, T., Kaneko, A., 2000. Eddy Field in the Japan Sea derived from Satellite Altimetric Data. Journal of Oceanography 56, 449–462.

Moriyasu, S., 1972. The Tsushima Current. In: Stommel, H., Yoshida, K. (Eds.), Kuroshio: Its Physical Aspects. University of Tokyo Press, Tokyo.

Munk, W.H., Cartwright, D.E., 1966. Tidal spectroscopy and prediction. Philosophical Transactions of the Royal Society of London 259, 533–581.

Naganuma, K., 1977. The oceanographic fluctuations in the Japan Sea. Mar. Sci. (Kaiyo Kagaku) 9, 137–141 (in Japanese).

Naganuma, K., 1985. Fishing and oceanographic conditions in the Japan Sea. Umi to Sora 60, 89–103 (in Japanese).

Park, J.-H., Watts, D.R., 2005. Response of the Southwestern Japan/East Sea to the Atmospheric pressure. Deep-Sea Research II, this issue [doi:10.1016/j.dsr2.2003.08.007].

Preller, R.H., Hogan, P.J., 1998. Oceanography of the Sea of Okhotsk and the Japan/East Sea. In: Robinson, A.R., Brink, K.H. (Eds.), The Sea. vol. 11, Wiley, New York.

Ramp, S.R., Barr, F.L., Ashjian, C.J., Talley, L.D., 2005. The upper-ocean circulation in the Ulleung Basin during June–July 1999. JGR-Oceans, submitted.

Senjyu, T., 1999. The Japan Sea intermediate water; its characteristics and circulation. Journal of Oceanography 55, 111–122.

Suda, K., Hidaka, K., 1932. The results of the oceanographical observations aboard R.M.S. Syunpu Maru in the southern part of the Sea of Japan in the summer of 1929. Journal of Oceanography Imperial Marine Observations 3, 291–375 (in Japanese).

Sugimoto, T., Tameishi, H., 1992. Warm-core rings, streamers and their role on the fisg ground formation around Japan. Deep Sea Research 39 (Suppl. 1), S183–S201.

Tanioka, K., 1968. On the East Korean Warm Current (Tosen Warm Current). The Oceanographical Magazine 20, 31–38.

Teague, W.J., Hwang, P.A., Jacobs, G.A., Book, J.W. Perkins, H.T., 2005a. Transport variability across the Korea/Tsushima Strait and the Tsushima Island Wake. Deep-Sea Research, this issue [doi:10.1016/j.dsr2.2003.07.021].

Teague, W.J., Tracey, K.L., Watts, D.R., Book, J.W., Chang, K.-I., Hogan, P.J., Mitchell, D.A., Suk, M.-S., Wimbush, M., Yoon, J.-H., 2005b. Observed deep circulation in the Ulleung Basin. Deep-Sea Research II, this issue [doi:10.1016/j.dsr2.2003.10.014].

Toba, Y., Tomizawa, K., Kurasawa, Y., Hanawa, K., 1982. Seasonal and year-to-year variability of the Tsushima–Tsugaru Warm Current system with its possible cause. La Mer 20, 41–51.

Uda, M., 1934. The results of simultaneous oceanographical investigations in the Japan Sea and its adjacent waters in May and June, 1932. Japan Imperial Fishery Experiment Stations 5, 57–190 (in Japanese).

Watts, D.R., Kontoyiannis, H., 1990. Deep-ocean bottom pressure measurement: drift removal and performance. Journal of Atmospheric and Oceanic Technology 7, 296–306.

Watts, D.R., Sun, C., Rintoul, S., 2001. A two-dimensional gravest empirical mode determined from hydrographic observations in the Subantarctic Front. Journal of Physical Oceanography 31, 2186–2209.

Yoon, J.-H., 1982. Numerical experiment on the circulation in the Japan Sea, Part 3. Mechanism of the nearshore branch of the Tsushima Current. Journal of the Oceanographical Society of Japan 38, 125–130.